

Synthesis and Characterization of the New Ternary Nitride (Fe_{0.8}W_{0.2})WN₂

Joel D. Houmes, Sandhya Deo, and Hans-Conrad zur Loye¹

Department of Chemistry, Massachusetts Institute of Technology, Cambridge, Massachusetts 02139

Received October 14, 1996; in revised form March 21, 1997; accepted March 25, 1997

The new layered ternary transition-metal nitride (Fe_{0.8}W_{0.2})WN₂ has been synthesized in a single-step ammonolysis of the transition-metal oxide precursor Fe₂(WO₄)₃. The nitride was characterized by powder X-ray diffraction, $a = 2.87 \text{ \AA}$, $c = 10.96 \text{ \AA}$. The proposed structure consists of alternating layers of MN₆ (M = W:Fe (1:4)) octahedra and M'N₆ (M' = W) trigonal prisms. Four-probe conductivity measurements indicate poor metallic conductivity with a very small temperature dependence. © 1997 Academic Press

INTRODUCTION

The synthesis of ternary and quaternary nitrides provides many interesting challenges to the synthetic solid state chemist. Because of its high bond energy (941 kJ/mol), the use of nitrogen gas requires high temperatures for a reaction to occur. This often results in the formation of intermetallic or simple binary nitrides. Recently, several groups have explored alternative synthetic routes, which have resulted in the synthesis of a number of new ternary and quaternary nitride materials (1–14).

The use of oxide precursors has been well documented as an experimentally simple and inexpensive method for the synthesis of a wide variety of nitride and oxynitride products (15–19). Of particular note are the recent syntheses of ternary nitrides containing two transition metals starting from the appropriate ternary oxide, demonstrating that complete conversion to a nitride product is possible (15, 18). Also, the ammonolysis of lithium molybdate and tungstate precursors yields ternary nitride materials with structures remarkably similar to those found in lithium intercalated molybdenum and tungsten dichalcogenides. In addition, ammonolysis reactions of ternary oxides containing rare earths (20–22) or vanadium (23) yield distinct oxynitride products.

¹To whom all correspondence should be addressed. Permanent Address: Department of Chemistry and Biochemistry, University of South Carolina, Columbia, SC 29208.

The use of oxide precursors offers the advantage of atomic-level mixing of the metals, which decreases the diffusion distance of the cations and may lower the temperature necessary for reaction. Also, the structure of the precursor may act as a template for product formation and yield phases unattainable by other synthetic routes. Currently we are investigating the use of transition-metal oxides as precursors to ternary transition-metal nitrides. In this paper, we report the synthesis, structure, and electronic characterization of (Fe_{0.8}W_{0.2})WN₂, which was synthesized from the ternary oxide precursor Fe₂(WO₄)₃.

EXPERIMENTAL

Fe₂(WO₄)₃ Synthesis

The iron tungstate precursor, Fe₂(WO₄)₃, was prepared by a method similar to that described by Kerr *et al.* (24) The compound was synthesized by dropwise addition of a 50 ml aqueous solution of iron chloride (Aldrich, 97%, 0.023 mol) to a 500 ml solution of sodium tungstate (Cerac, 99.9%, 0.034 mol). The solution was acidified to pH 3.6 by the addition of acetic acid. After addition, the solution was stirred for 1 hr and the yellow precipitate was isolated by vacuum filtration. The product was washed with two ~ 20 mL washings of water followed by a single ~ 20 mL washing with anhydrous ethanol. The solid was dried overnight and was found to be amorphous by powder X-ray diffraction.

Nitride Synthesis

The nitride, (Fe_{0.8}W_{0.2})WN₂, was synthesized by heating ~ 0.5 g of Fe₂(WO₄)₃ under flowing ammonia at 700°C for 96 hr with one intermediate grinding. (Caution: Ammonia is a corrosive, toxic gas which must be used in a properly ventilated area.) The precursor was placed into an alumina boat, which was then inserted into a flow-through reactor. The sample was heated at 5°C/min to 700°C and soaked for 48 hr under flowing ammonia gas (Airco, anhydrous 99.99%, 150 cm³/min). After 48 hr, the sample was cooled by

turning off the furnace and opening it. Once the sample had cooled to room temperature, it was removed from the system, ground, and reheated using the identical heating cycle. A pure product was obtained only over a narrow temperature range for a given flow rate. By trial and error, 700°C was found to be the reaction temperature that gave the cleanest, most crystalline product.

Characterization

X-ray diffraction. Powder X-ray diffraction patterns were collected using a Siemens D5000 diffractometer operating at 40 kV and 45 mA with $\text{CuK}\alpha$ radiation. Qualitative phase analysis of the oxide precursor and the nitride product was performed using a continuous scan. Pattern indexing was carried out using the indexing program TREOR (25). The lattice parameters and theoretical powder patterns were calculated using the NRCVAX crystal structure system (26). A step-scanned diffraction pattern of ($\text{Fe}_{0.8}\text{W}_{0.2}$) WN_2 ($5^\circ \leq 2\theta \leq 118^\circ$, 0.05° steps) was used for Rietveld refinements, which were performed using the General Structure Analysis System, GSAS. (27)

Elemental analysis. The nitrogen content of the nitride was determined by nitrogen combustion analysis (Galbraith Laboratories Inc.) ($N = 9.95$ wt%). The oxygen impurity level was determined by vacuum fusion analysis (LECO Oxygen 2.26 wt% Mass Materials Research). The metal ratio of the nitride product was determined by ICP (Galbraith Laboratories Inc.). The ratio $(\text{Fe wt}\%)_{\text{obs}}/(\text{W wt}\%)_{\text{obs}} = 0.22$ agrees with the expected ratio $(\text{Fe wt}\%)_{\text{theor}}/(\text{W wt}\%)_{\text{theor}} = 0.20$. Together, these yield an overall composition of ($\text{Fe}_{0.8}\text{W}_{0.2}$) $\text{WN}_{2.15}\text{O}_{0.4}$. We were unable to determine whether the oxygen impurity is due to unreacted starting material or surface oxidation.

Conductivity measurements. Temperature-dependent two- and four-probe resistance measurements were performed on pressed pellets using a Keithly 236 source measure unit and a Janis closed-cycle refrigerator (Model ccs-200) by measuring the voltage at a constant current of 1 mA. Pellets were pressed at 5000 psi in air.

RESULTS AND DISCUSSION

The product of the ammonolysis of $\text{Fe}_2(\text{WO}_4)_3$, $\text{Fe}_{0.8}\text{W}_{1.2}\text{N}_2$, is a black crystalline powder that is stable with respect to air and moisture. The nitride was decomposed by heating in oxygen at 900°C to yield Fe_2O_3 and WO_3 . The observed mass gain, 12.40 wt% (Fig. 1), was smaller than the theoretical mass gain of 14.26% for the oxidation of $\text{Fe}_{0.8}\text{W}_{1.2}\text{N}_2$ to $0.4\text{Fe}_2\text{O}_3$ and 1.2WO_3 , which indicates the presence of residual oxygen in the nitride. The mass gain corresponds to a starting composition of $\text{Fe}_{0.8}\text{W}_{1.2}\text{N}_2$ with 2.1 wt% residual oxygen, which is close

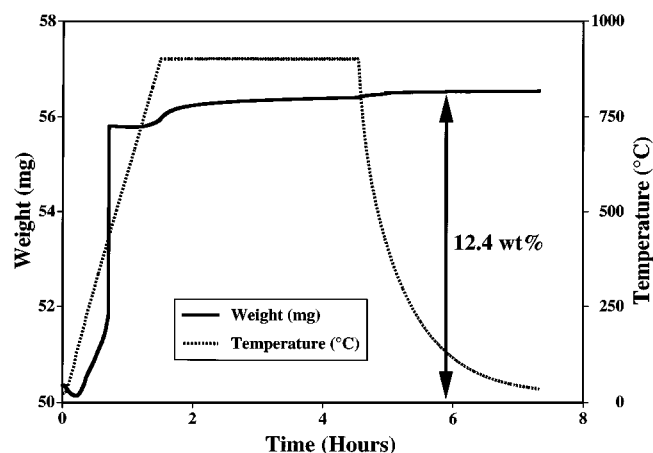


FIG. 1. Thermogravimetric data for ($\text{Fe}_{0.8}\text{W}_{0.2}$) WN_2 heated to 900°C in flowing O_2 .

to the value of the oxygen content obtained from oxygen analysis (2.26 wt%).

Indexing of the powder X-ray diffraction data for $\text{Fe}_{0.8}\text{W}_{1.2}\text{N}_2$ gave a hexagonal unit cell of approximately $a = 2.87 \text{ \AA}$, $c = 10.96 \text{ \AA}$. Based on systematic absences and experience with other ternary transition-metal nitrides of similar composition, the space group $P6_3/mmc$ was chosen for Rietveld refinement. A powder pattern was calculated using this space group and found to be in agreement with the observed data. Given the similarities in elemental composition and diffraction pattern, the structure of ($\text{Fe}_{0.8}\text{Mo}_{0.2}$) MoN_2 (15) was used as a starting point for a Rietveld refinement of the data.

Despite our success in using Rietveld refinement as a structural characterization tool for nitrides of similar composition and structure, refinements of $\text{Fe}_{0.8}\text{W}_{1.2}\text{N}_2$ failed to converge with acceptable goodness of fit values. Close inspection of the powder X-ray diffraction data (Fig. 2a) reveals the difficulty in refining this structure. The diffraction peaks of $\text{Fe}_{0.8}\text{W}_{1.2}\text{N}_2$ can be divided into two groups. One includes the particularly broad $00l$ reflections, while the other includes the particularly narrow $h00$ and $hk0$ reflections. Additional heating of up to 96 hr does not result in any significant sharpening of the broader peaks. The presence of two disparate peak shapes makes refinement of the powder X-ray diffraction data problematic, since the GSAS structure refinement package does not handle two peak shapes within the same phase well. Several unsuccessful attempts were made to account for the peak width disparity. Refinement of anisotropic profile values only resulted in a slight improvement of the goodness of fit values. However, neither set of peaks was fit well. Also, an attempt was made to refine the phase as two histograms, one of which contained only the narrow peaks while the other

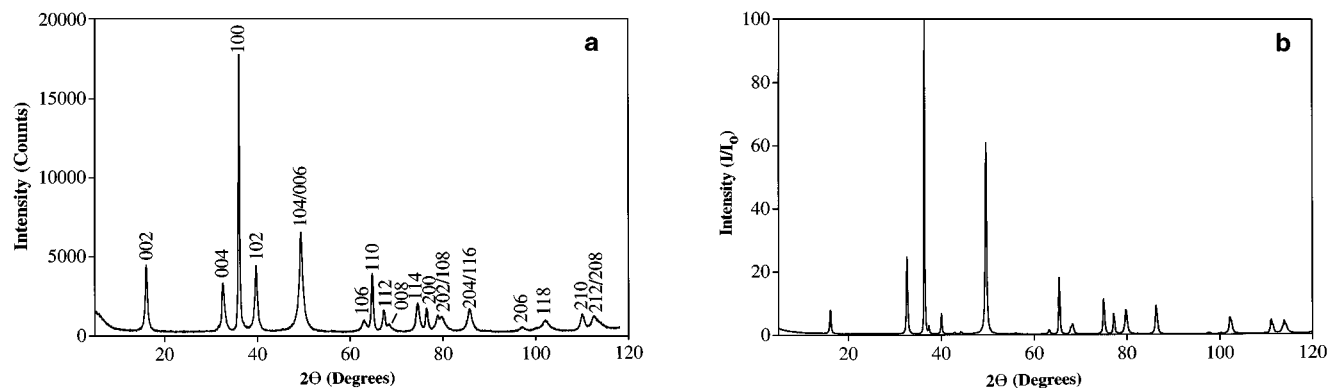


FIG. 2. (a) Powder X-ray diffraction pattern of $(\text{Fe}_{0.8}\text{W}_{0.2})\text{WN}_2$. Numbers over peaks indicate hkl values. (b) Powder X-ray diffraction pattern of $(\text{Fe}_{0.8}\text{Mo}_{0.2})\text{MoN}_2$ for comparison.

contained only the broader ones. However, this approach did not yield any significant improvement in the fit.

Despite the difficulties in refining the structure of $\text{Fe}_{0.8}\text{W}_{1.2}\text{N}_2$, we propose, based on the similarities of the powder diffraction patterns (Figs. 2a and 2b), that the structure is identical or closely related to that of $\text{Fe}_{0.8}\text{Mo}_{1.2}\text{N}_2$ (15). The proposed atomic positions for $\text{Fe}_{0.8}\text{W}_{1.2}\text{N}_2$ are listed in Table 1. The structure (Fig. 3) consists of alternating layers of edge-shared octahedra and trigonal prisms, where the octahedra and trigonal prisms are face-shared in the c direction. The arrangement of the nitrogen and metal atoms can be represented by $AcAcBcBcA$, where A and B represent the close-packed nitrogen atoms with significant disorder between the two positions and c represents the metal atoms. The trigonal prismatic layer is occupied exclusively by tungsten, while the octahedral layer contains iron and molybdenum randomly distributed in an approximately 4:1 ratio. The composition can be more accurately written as $(\text{Fe}_{0.8}\text{W}_{0.2})\text{WN}_2$. In this structure, the two narrow peaks have $[hkl]$ $l = 0$, while for all other peaks $l \neq 0$. This variation in peak FWHM is indicative of significant structural disorder along the c -axis, which could take the form of a shifting of the WN_6 trigonal prismatic slabs, a disorder of the metal positions, or a shifting of the nitrogen positions.

Patterson maps constructed from the powder X-ray diffraction step-scan data in space group $P1$ provide some

insight into the cause of the peak broadening. Figure 4 shows the electron density in the $[0\ 0\ 5/8]$ plane, which contains the nitrogen atoms. The electron density forms a pseudo-6-fold symmetry axis around the c -axis, with almost identical electron density at each site. The even distribution of electron density is repeated in every plane $[0\ 0\ n/8]$ ($n = 1-8$). This is in contrast to other ternary transition-metal nitrides which exhibit much more ordered nitrogen positions with 3-fold symmetry around the c -axis. The distance between sites in the Patterson diffraction map is too small to allow for total occupation of all the sites. The

TABLE 1
Proposed Atomic Positions for $(\text{Fe}_{0.8}\text{W}_{0.2})\text{WN}_2$

Atom	Wyckoff	x	y	z	Occupancy
Fe	$2b$	0	0	$1/4$	0.8
W	$2b$	0	0	$1/4$	0.2
W	$2a$	0	0	0	1.0
N	$4f$	$1/3$	$2/3$	$1/8$	1.0

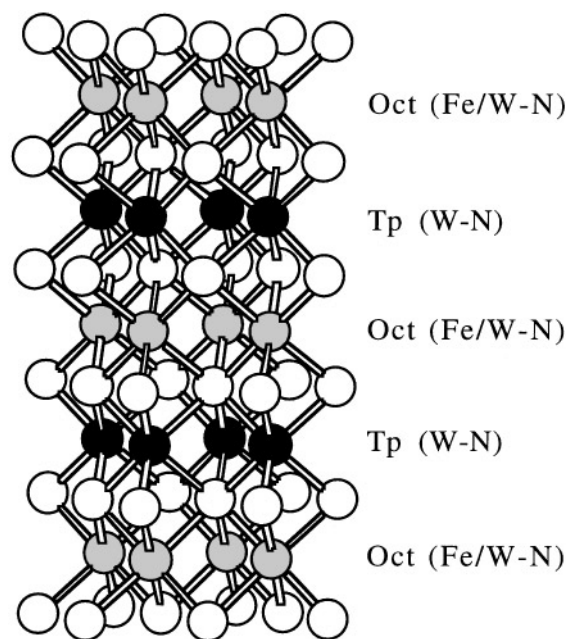


FIG. 3. Proposed structure of $(\text{Fe}_{0.8}\text{W}_{0.2})\text{WN}_2$. Gray, Fe/W; Black, W; and White, Nitrogen. The arrangement of the nitrogen and metal atoms can be represented by $AcAcBcBcA$, where A and B represent the close-packed nitrogen atoms and c the metal atoms.

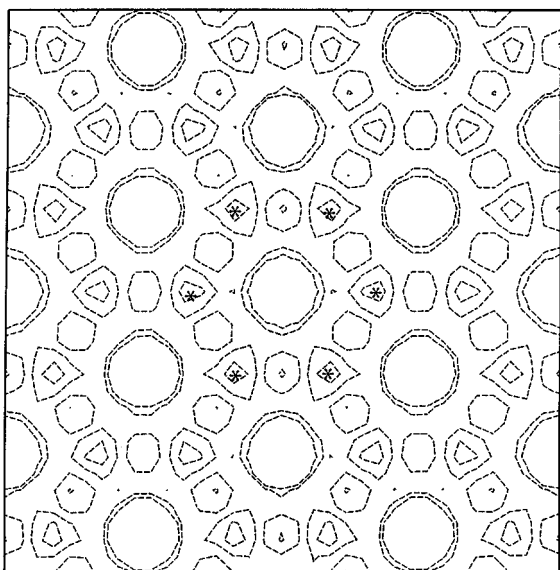


FIG. 4. Patterson map of $(\text{Fe}_{0.8}\text{W}_{0.2})\text{WN}_2$ in the $0\ 0\ 5/8$ plane. The asterisks indicate possible positions for N.

partial occupancy therefore required could reasonably arise through severe disorder of the nitrogen planes caused by stacking faults along the c -axis.

The presence of 6-fold symmetry of nitrogen electron density around the c -axis indicates an almost complete disorder along the c -axis between the A and B positions of the nitrogen close-packed planes. Such disorder could exist while still maintaining the integrity of the highly covalent WN_2 sheets and without significantly affecting the unit cell by translation of one or more nitrogen close-packed planes by $[1/3\ 1/3\ 0]$. Such translation could be easily rationalized by the presence of tungsten in the iron layer of the structure. Tungsten would prefer trigonal prismatic coordination over octahedral and if the concentration of tungsten in the octahedral layer is sufficiently large, this preference could be accommodated by translation of one of the adjacent nitrogen planes $[1/3\ 1/3\ 0]$, creating the necessary structural disorder responsible for the broadening of the peaks with $[hkl]\ l \neq 0$.

Despite the difficulty in satisfactorily refining the structure of $(\text{Fe}_{0.8}\text{W}_{0.2})\text{WN}_2$, the electronic properties exhibited by the material are consistent with other members of this family of compounds. Four-probe dc conductivity measurements between 17 and 295 K indicate that the conductivity of $(\text{Fe}_{0.8}\text{W}_{0.2})\text{WN}_2$ exhibits a very small temperature dependence (Fig. 5). Similar conductivity data have also been observed in the structurally related ternary nitrides LiMoN_2 , MnMoN_2 , $\alpha, \beta\text{-MnWN}_2$, and FeWN_2 . The proposed layered structure of $(\text{Fe}_{0.8}\text{W}_{0.2})\text{WN}_2$ suggests that some anisotropy should be exhibited in the electrical con-

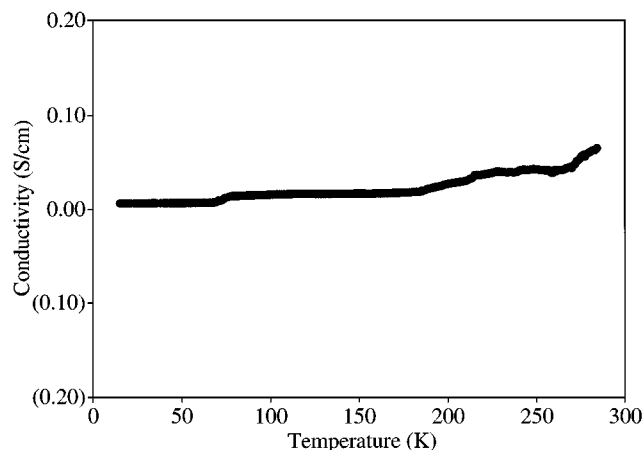


FIG. 5. Electronic conductivity of $(\text{Fe}_{0.8}\text{W}_{0.2})\text{WN}_2$ exhibiting essentially temperature-independent metallic behavior.

ductivity of the sample. Since the measurement was performed on a pressed pellet, the data represent an average of all orientations plus a contribution from grain boundary resistance, which may significantly decrease the conductivity. Therefore, our data should represent a lower limit of the conductivity of $(\text{Fe}_{0.8}\text{W}_{0.2})\text{WN}_2$.

SUMMARY

The new layered ternary transition-metal nitride $(\text{Fe}_{0.8}\text{W}_{0.2})\text{WN}_2$ has been synthesized by ammonolysis of the transition-metal oxide precursor, $\text{Fe}_2(\text{WO}_4)_3$. Powder X-ray data were collected and were consistent with a proposed structure, consisting of alternating layers of $M\text{N}_6$ ($M = \text{W}:\text{Fe}\ (1:4)$) octahedra and $M'\text{N}_6$ ($M' = \text{W}$) trigonal prisms. Four-probe conductivity measurements indicate that the material has poor metallic conductivity with a very small temperature dependence. The structure and properties of this compound are similar to those found for the isostructural ternary nitrides FeWN_2 and $(\text{Fe}_{0.8}\text{Mo}_{0.2})\text{MoN}_2$.

ACKNOWLEDGMENTS

Acknowledgment is made to the donors of The Petroleum Research Fund, administered by the American Chemical Society, for partial support. J.D.H. acknowledges 3M for support.

REFERENCES

1. A. Gudat, R. Kniep, A. Rabenau, W. Bronger, and U. Ruschewitz, *J. Less-Common Met.* **161**, 31 (1990).
2. A. Gudat, R. Kniep, and A. Rabenau, *Thermochim. Acta* **160**, 49 (1990).
3. R. L. LaDuca and P. T. Wolczanski, *Inorg. Chem.* **31**, 1311 (1992).
4. J. B. Wiley and R. B. Kaner, *Science* **255**, 1093 (1992).

5. U. Zachwieja and H. Jacobs, *Eur. J. Solid State Inorg. Chem.* **28**, 1055 (1991).
6. M. M. B. Holl, P. T. Wolczanski, and G. D. Van Duyne, *J. Am. Chem. Soc.* **112**, 7989 (1990).
7. A. Gudat, W. Milius, S. Haag, R. Kniep, and A. Rabenau, *J. Less-Common Met.* **168**, 305 (1991).
8. A. Gudat, R. Kniep, and A. Rabenau, *Angew. Chem.* **103**, 217 (1991).
9. P. Höhn and R. Kniep, *Z. Naturforsch.* **47**, 477 (1992).
10. P. Höhn, S. Haag, W. Milius, and R. Kniep, *Angew. Chem.* **103**, 874 (1991).
11. A. Gudat and R. Kniep, *J. Alloys Compd.* **179**, 333 (1992).
12. D. S. Bem, C. P. Gibson, and H.-C. zur Loye, *Chem. Mater.* **5**, 397 (1993).
13. D. S. Bem and H.-C. zur Loye, *J. Solid State Chem.* **104**, 467 (1993).
14. J. Houmes, D. Bem, and H.-C. zur Loye, *Mater. Res. Soc. Symp. Proc.* **327**, 153 (1994).
15. D. S. Bem, H. P. Olsen, and H.-C. zur Loye, *Chem. Mater.* **7**, 1824 (1995).
16. S. H. Elder, F. J. DiSalvo, and L. H. Doerrer, *Chem. Mater.* **4**, 928 (1992).
17. P. Subramanya Herle, M. S. Hegde, N. Y. Vasanthacharya, J. Gopalakrishnan, and G. N. Subbanna, *J. Solid State Chem.* **112**, 208 (1994).
18. D. S. Bem, C. M. Lampe-Önnerud, H. P. Olsen, and H.-C. zur Loye, *Inorg. Chem.* **35**, 581 (1996).
19. R. Marchand, Y. Laurent, J. Guyader, P. L'Haridon, and P. Verdier, *J. Eur. Ceram. Soc.* **8**, 197 (1991).
20. R. Marchand, P. Antoine, and Y. Laurent, *J. Solid State Chem.* **107**, 34 (1993).
21. F. Pors, R. Marchand, and Y. Laurent, *J. Solid State Chem.* **107**, 39 (1993).
22. P. Bacher *et al.*, *J. Solid State Chem.* **77**, 67 (1988).
23. C. C. Yu and S. T. Oyama, *J. Solid State Chem.* **116**, 205 (1995).
24. P. F. Kerr, A. W. Thomas, and A. M. Langer, *Am. Mineral.* **48**, 14 (1963).
25. P. E. Werner, L. Eriksson, and M. Westdahl, *J. Appl. Crystallogr.* **18**, 367 (1985).
26. A. C. Larson *et al.*, "NRCVAX Crystal Structure System" (P. S. White, Ed.), Chemistry Division, NRC, Ottawa, Canada, K1A 0R6.
27. A. C. Larson and R. B. von Dreele, "General Structure Analysis System, GSAS." Los Alamos, NM, 1990.